

Rational design of potent and selective NH-linked aryl/heteroaryl cathepsin K inhibitors

Joël Robichaud,^{a,*} Christopher Bayly,^{a,*} Renata Oballa,^a Peppi Prasit,^a
Christophe Mellon,^a Jean-Pierre Falguyret,^b M. David Percival,^b
Gregg Wesolowski^c and Sevgi B. Rodan^c

^aDepartment of Medicinal Chemistry, Merck Frosst Centre for Therapeutic Research, 16711 TransCanada Highway, Kirkland, QC, Canada H9H 3L1

^bDepartment of Biochemistry and Molecular Biology, Merck Frosst Centre for Therapeutic Research, 16711 TransCanada Highway, Kirkland, QC, Canada H9H 3L1

^cDepartment of Bone Biology and Osteoporosis, Merck Research Laboratories, West Point, PA, USA

Received 28 April 2004; revised 28 May 2004; accepted 28 May 2004

Available online 19 June 2004

Abstract—Prior reports from our laboratories have identified the nonpeptidic inhibitor **2** as a potent and selective Cathepsin K (Cat K) inhibitor. Modelling studies suggested that the introduction of a NH linker between the P3 aryl and P2 leucinamide moieties would allow the formation of a H-bond with the Gly66 residue of Cat K, hopefully increasing potency. Aniline **4** was thus synthesized and showed improved potency over its predecessor **2**. Further modelling concluded that a 2-substituted five membered ring could more adequately place the P3 moiety of **4** into the S3 pocket of Cat K. The synthesis of the 2-substituted thiophene **5** confirmed this hypothesis by displaying a slight increase in potency against Cat K (>10-fold increase in potency vs **2**) and a good selectivity profile against Cathepsins B, L, and S. This rationally designed inhibitor **5** also displayed increased potency in a functional bone resorption assay (10 nM) versus **2** (95 nM).

© 2004 Elsevier Ltd. All rights reserved.

1. Introduction

Extensive research in the field of bone biology in recent years has yielded new discoveries that have further enhanced our appreciation of the intricate mechanisms governing bone turnover. These processes are mediated by highly specialized cells named osteoblasts and osteoclasts that are responsible for bone tissue formation and resorption, respectively. Much of this research interest was fueled by the hope that the understanding of these processes would identify potential targets for therapeutic intervention for degenerative diseases such as osteoporosis.

Cathepsin K (Cat K) is a cysteine protease that is highly expressed by osteoclasts and has been shown to be a key enzyme involved in bone resorption.¹ Secreted in the extracellular acidic lacunae at the interface of the osteoclast and bone tissue, the enzyme's primarily role consists of type I collagen degradation, one of the main

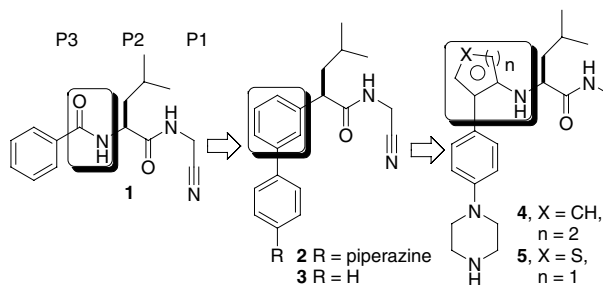


Figure 1. Amide bond replacement of dipeptide **1** affords biaryls **2** and **3**, which are further modified to the NH-linked biaryl **4** and heteroaryl **5** to reintroduce a favorable H-bond interaction with the Cat K enzyme.

Keywords: Cathepsin K inhibitors; Bone resorption; Modelling; Biaryl piperazine.

* Corresponding authors. Tel.: +1-514-4283665; fax: +1-514-4284900; e-mail: joel_robichaud@merck.com

constituents of bone matrix. It has been suggested that the inhibition of Cat K could slow bone resorption and it appears that Cat K represents a promising therapeutic target for the treatment of osteoporosis.²

2. Results

As previously reported,³ work in our laboratories to achieve these goals focused on reducing the peptidic character of **1**⁴ by replacing its P2-P3 amide bond with a phenyl to afford biaryl **3** (Fig. 1). The resulting inhibitor **3** retained potency while displaying an improved selectivity profile. Further SAR around the biaryl core of **3** led to the discovery of the potent and selective Cat K inhibitor **2** (humanized rabbit IC₅₀ = 11 nM).

However, this phenyl replacement removes the H-bond donated by the P2-P3 amide of **1** to the backbone oxygen of Gly66 in the enzyme (Fig. 2), instead leaving this enzyme oxygen unpaired.⁵ This presumably incurs a desolvation penalty to binding. The goal of this publication is to outline our efforts to re-engineer our inhibitors with this favorable H-bonding interaction, thus leading us to inhibitors such as **4** and **5**.⁶

Modelling studies⁸ suggested that the insertion of a NH H-bond donor between P2 and the biaryl core could rectify this problem. Molecular dynamics results on fully-solvated covalently-bound inhibitor/enzyme complex showed that the aniline NH would introduce a correctly-placed nonbasic H-bond donor while retaining the nonpeptidic P2-P3 linker of this series (Fig. 3). A good overall H-bonding configuration and a good overall fit of the inhibitor was maintained. The P3 piperazine analog to **3** would still lie in P3, although with a different orientation (data not shown).

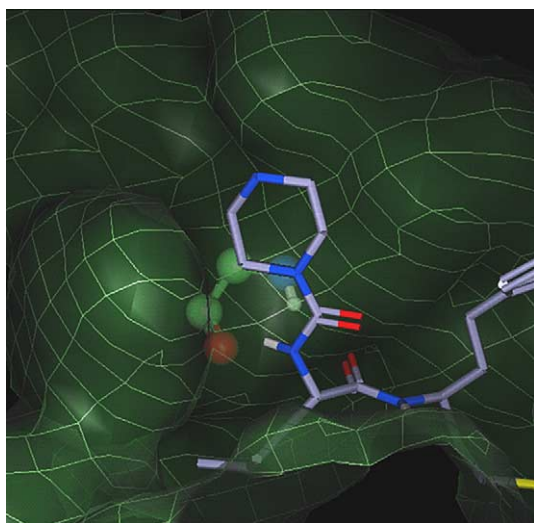


Figure 2. The crystal structure of the active site of Cat K with bound peptidomimetic inhibitor having a P2-P3 amide similar to **1**.⁷ The H-bond between the P2-P3 amide NH and the backbone oxygen of Gly66 (visible underneath the active site surface) is shown as a dashed yellow line. This irreversible vinylsulfone inhibitor covalently binds to the Cys25 (not shown), the P1-P3 portion adopting a peptide-like binding orientation.

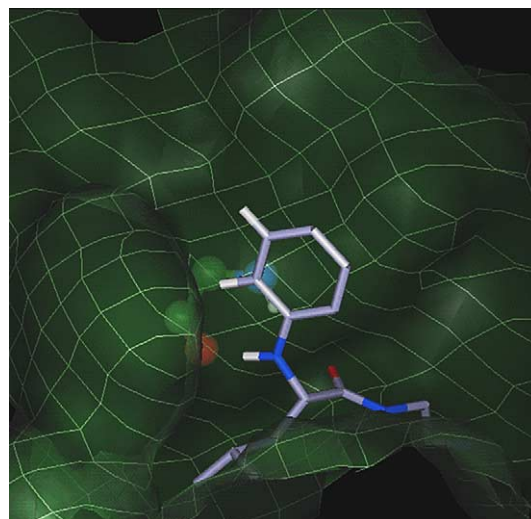


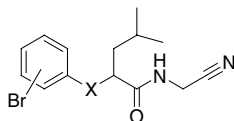
Figure 3. The average structure resulting from molecular dynamics of a simple aniline linker (desbromo-**6**) in Cat K. The H-bond between the inhibitor P2-P3 NH and the backbone oxygen of Gly66 (visible under the active site surface) is shown as a dashed yellow line. Hydrogens depict *ortho*- and *meta*-substitution positions of the aniline; neither is optimal.

An aminoaryl linker would substantially change the orientation of the P3-fragment compared to the simple phenyl linker so the *meta*-substitution of the biaryl core would have to be re-examined. The aniline molecular dynamics result suggested that neither *ortho* nor *meta*-substitution appeared optimal: without allowing the aniline phenyl to shift, *ortho*-substitution would sterically clash with S3 while *meta*-substitution would be directed slightly out of the S3 subsite into solvent.

Allowing for some degree of movement of the aniline phenyl, both *ortho*- and *meta*-substitutions on the phenyl (depicted by the hydrogen substitutions on the phenyl in Fig. 3) could be substituted to access P3. Also, to evaluate whether the effect on potency of inserting an NH linker was attributable to H-bonding or simply a geometric consequence of the added atom, CH₂, O, and S linkers were also tested. In addition to removing the H-bond, these replacements also examine the effects of modifying the coplanarity of the phenyl with the X-CH bond from P2: O will favor a coplanar structure (as with the aniline), CH₂ will favor perpendicular, whereas S will favor neither.

The biological results obtained (Table 1) from the variously linked aryl bromides were in accordance with the modelling hypothesis. The NH linker showed markedly increased potency compared to any other linkers, irrespective of the substitution on the phenyl ring. The most potent compounds proved to be the *ortho*- and *meta*-substituted NH-linked aryl bromides **6** and **7** which displayed potencies of 54 and 72 nM against Cat K, respectively.

The CH₂ and O linkers are the most similar to NH in terms of size and bond lengths, differing mainly in their H-bonding capability, CH₂ being neutral and O being a

Table 1. Inhibition of Cat K with NH, CH₂, O, and S-linked inhibitors

Linker X	<i>ortho</i> -Isomer	Cat K IC ₅₀ (nM) ^a	<i>meta</i> -Isomer	Cat K IC ₅₀ (nM) ^a	<i>para</i> -Isomer	Cat K IC ₅₀ (nM) ^a
NH ^b	6	54	7	72	8	208
CH ₂	9	2352	10	3394	11	2349
O	12	1147	13	1475	14	2999
S	15	433	16	684	17	675

^a IC₅₀ values represent an average of at least $n = 2$, variation between obtained values were within 2-fold. Humanized rabbit Cat K was used (see Ref. 3a for conditions used).

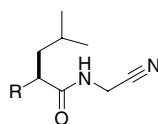
^b Aniline compounds (**6**, **7**, and **8**) are chiral and of *S*-configuration.

hydrogen bond acceptor. The >20-fold improvement of the NH compared to these two linkers affirms the importance of the H-bond to Gly66. The only other series registering potencies below 1 μM was the *S*-linked aryl bromides.

Aware that the extent of substitution in P3 may have a dramatic influence on potency and selectivity, we decided to introduce our previously optimized phenyl piperazine P3 moiety³ onto our three promising NH-linked aryl bromides (**6**, **7**, and **8**). Closely tracking the SAR of the aryl bromide series, the most potent inhibitors proved to be the *ortho*- and *meta*-substituted biphenyl piperazines **4** and **18** (Table 2) with potencies

of 3 and 2 nM, respectively, against Cat K. In contrast, the *para*-substituted phenyl piperazine **19** displayed a potency of 27 nM. While the selectivity profile of these two NH-linked biaryl piperazines **4** and **18** against Cathepsins B, L, and S was lacking in comparison to the biaryl piperazine **2**, the potency of the *ortho*-isomer **4** in the functional bone resorption assay⁹ was improved (IC₅₀ = 9 nM, compared to 95 nM for **2**). The *meta*-isomer **18** on the other hand showed comparatively less potency in this functional assay (IC₅₀ = 61 nM).

Re-examination of the modelling studies in light of these experimental results suggested that the similar potencies of *ortho*- and *meta*-substitutions represented extremes of

Table 2. Inhibition of Cat K, B, L, and S by other *N*-linked inhibitors

R	Compd	IC ₅₀ (nM)				Bone res. ^c
		Cat K ^a	Cat B ^b	Cat L ^b	Cat S ^b	
	2	11 ^d	3950	3725	2010	95
	<i>ortho</i> 4	3	1812	2101	158	9
	<i>meta</i> 18	2	93	108	24	61
	<i>para</i> 19	27	26	115	34	37
	20	43	158	458	897	71
	5	1 ^d	123	352	102	10

^a IC₅₀ values represent an average of at least $n = 2$, variation between obtained values were within 2-fold. Humanized rabbit Cat K was used (see Ref. 3a for conditions used).

^b Human enzyme was used for these assays (see Ref. 3a for conditions used).

^c See Ref. 9 for assay conditions.

^d Compound **2** is 3 nM against human Cat K, whereas compound **2** is 0.2 nM against human Cat K.

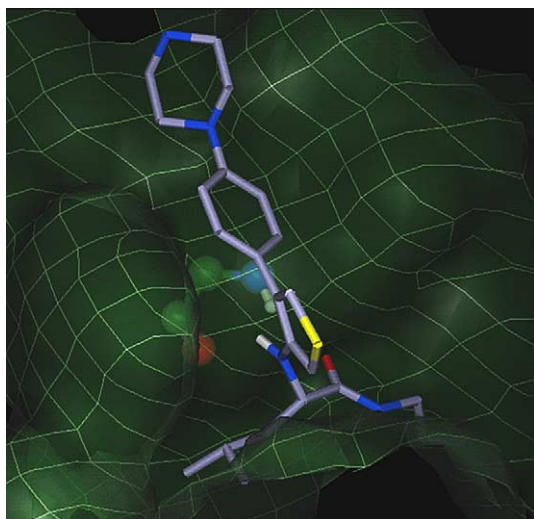


Figure 4. The average structure resulting from molecular dynamics of **5** in Cat K. The hydrogen bond between the inhibitor P2-P3 amine NH and the backbone oxygen of Gly66 (visible underneath the active site surface) is shown as a dashed yellow line.

allowed angles of P3 substitution, and that an intermediate angle might be better. Since the angle between 1,2-substitution on a five-membered heteroaromatic ring (around 72°) falls in between that of *ortho* (60°) and *meta* (120°) substitution on a phenyl ring, replacing the aniline phenyl with a five-membered heteroaryl moiety (i.e. thiophene) might yield improved potency by allowing the P3 phenyl piperazine to sit better in S3 (see Fig. 4).

To test this hypothesis both the thiophene bromide **20** and the corresponding phenyl piperazine **5** were prepared (Table 2). While the simple bromo-substituted inhibitor **20** (43 nM against Cat K) showed no significant improvement over the *ortho*-substituted bromo-aniline **6** (54 nM), the fully elaborated phenyl piperazine derivative **5** displayed a slightly improved potency of 1 nM against humanized rabbit Cat K (0.2 nM against human Cat K) and a good selectivity profile against Cathepsins B, L, and S (123-fold, 352-fold, and 102-fold, respectively). Importantly, this potent inhibitor **5** also displayed very good potency ($IC_{50} = 10$ nM) in the functional bone resorption assay.

3. Conclusion

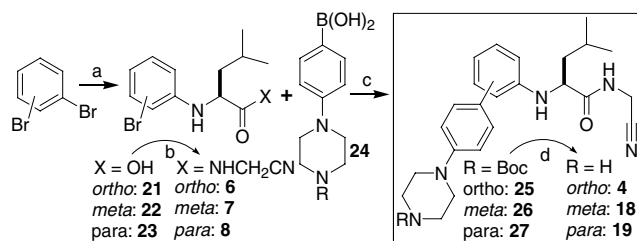
In summary, reintroducing a H-bond donating NH linker in our nonpeptidic inhibitors led to anilines **4** and **18**, which showed improved potencies over a previously disclosed biaryl piperazine inhibitor **2**. Further refinement of the geometrical biaryl scaffold of **4** and **18** led to the rational design of thiophene **5** which displayed good selectivity against Cathepsins B, L, and S and a 10-fold improvement in potency against Cat K in comparison to **2**. Inhibitor **5** also showed very good potency ($IC_{50} = 10$ nM) in the functional bone resorption assay. Further SAR in this series is ongoing and will be disclosed in due course.

4. Chemistry

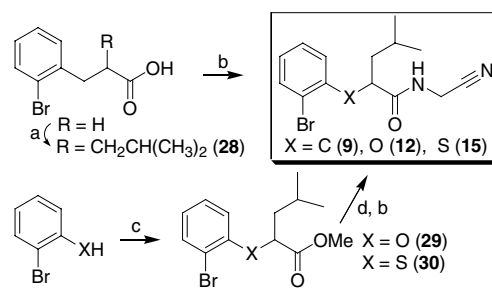
The synthesis of the NH-linked biaryls (Scheme 1) began with the copper-catalyzed cross-coupling reaction of the required dibromobenzene (*ortho*, *meta*, and *para*) with L-leucine in DMF under basic conditions.¹⁰ This sequence afforded the desired aniline-acids **21**, **22**, and **23** in good yields, which were coupled with aminoacetonitrile hydrochloride to afford the corresponding isomeric amides **6**, **7**, and **8**. Suzuki cross-coupling of these aryl bromides with boronic acid **24**³ afforded the desired Boc-protected piperazine biaryls **25**, **26**, and **27**, which were carefully deprotected³ using methanesulfonic acid in dry THF to yield the three positional isomers **4**, **18**, and **19**.

The synthesis of the C-linked biaryls (Scheme 2) began with the commercially available 3-(2-bromophenyl) propionic acid, which was deprotonated with LDA and alkylated with 1-iodo-2-methylpropane to yield the desired carboxylic acid **28**, which was then converted to the desired amidoacetonitrile **9** according to the usual PyBOP coupling reaction (the same route was used for the *meta*- and *para*-isomers, all compounds were prepared as racemic mixtures).

The synthetic route utilized for the preparation of the *O* and *S*-linked biaryls was analogous for both families of compounds. The commercial 2-bromophenol and 2-bromothiophenol (Scheme 2) were deprotonated with NaH and alkylated with methyl 2-bromo-4-methyl-



Scheme 1. Synthetic route to NH-linked derivatives. Reagents and conditions: (a) (L)-leucine, K_2CO_3 , CuI (cat), DMF, Δ ; (b) $HCl \cdot H_2NCH_2CN$, PyBOP, Et_3N , DMF; (c) aq Na_2CO_3 , $PdCl_2(dppf)$, DMF, $85-90^\circ C$; (d) $MeSO_3H$, THF.



Scheme 2. General synthetic route to the CH_2 , *O*, and *S*-linked analogs. Reagents and conditions: (a) LDA, THF, $0^\circ C$, then 1-iodo-2-methylpropane, rt; (b) $HCl \cdot H_2NCH_2CN$, PyBOP, Et_3N , DMF; (c) NaH (60%), THF, then methyl 2-bromo-4-methylpentanoate; (d) LiOH, MeOH.

pentanoate¹¹ to afford the desired ether **29** and thioether **30**. The resulting esters were converted to the *O* and *S*-linked nitrile inhibitors **12** and **15** as described in Scheme 2 (the same route was used for the *meta*- and *para*-isomers, all compounds were synthesized as racemic mixtures).

Access to the NH-linked thiophenes **20** and **5** was accomplished starting from commercially available 3,4-dibromothiophene and using the same synthetic route described in Scheme 1.

References and notes

- Motyckova, G.; Fisher, D. E. *Curr. Mol. Med.* **2002**, *2*, 407.
- For recent reviews on this subject see: (a) Stroup, G. B.; Lark, M. W.; Veber, D. F.; Bhattacharyya, A.; Blake, S.; Dare, L. C.; Erhard, K. F.; Hoffman, S. J.; James, I. E.; Marquis, R. W.; Ru, Y.; Vasko-Moser, J. A.; Smith, B. R.; Tomaszek, T.; Gowen, M. *J. Bone Miner. Res.* **2001**, *16*, 1739; (b) Yamashita, D. S.; Dodds, R. A. *Curr. Pharm. Des.* **2001**, *6*, 1.
- (a) Robichaud, J.; Oballa, R.; Prasit, P.; Falguyret, J.-P.; Percival, M. D.; Wesolowski, G.; Rodan, S. B.; Kimmel, D.; Johnson, C.; Bryant, C.; Venkatraman, S.; Setti, E.; Mendoca, R.; Palmer, J. T. *J. Med. Chem.* **2003**, *46*, 3709; (b) Chen, C.-Y.; Dagneau, P.; Grabowski, E. J. J.; Oballa, R.; O'Shea, P.; Prasit, P.; Robichaud, J.; Tillyer, R.; Wang, X. *J. Org. Chem.* **2003**, *68*, 2633.
- Suzue, S.; Irikura, T. *Chem. Pharm. Bull.* **1968**, *16*, 1417.
- DesJarlais, R. L.; Yamashita, D. S.; Oh, H.-J.; Uzinskas, I. N.; Erhard, K. F.; Allen, A. C.; Haltiwanger, R. C.; Zhao, B.; Smith, W. W.; Abdel-Meguid, S. A.; D'Alessio, K.; Janson, C. A.; McQueney, M. S.; Tomaszek, T. A.; Levy, M. A.; Veber, D. F. *J. Am. Chem. Soc.* **1998**, *120*, 9114.
- For a similar approach, see: Greenspan, P. D.; Clark, K. L.; Cowen, S. D.; McQuire, L. W.; Tommasi, R. A.; Farley, D. L.; Quadros, E.; Coppa, D. E.; Du, Z.; Fang, Z.; Zhou, H.; Doughty, J.; Toscano, K. T.; Wigg, A. M.; Zhou, S. *Bioorg. Med. Chem. Lett.* **2003**, *13*, 4121.
- McGrath, M. E.; Klaus, J. L.; Barnes, M. G.; Bromme, D. *Nat. Struct. Biol.* **1997**, *4*, 105, PDB entry 1MEM.
- Case, D. A.; Pearlman, D. A.; Caldwell, J. W.; Cheatham, T. E., III; Ross, W. S.; Simmerling, C. L.; Darden, T. A.; Merz, K. M.; Stanton, R. V.; Cheng, A. L.; Vincent, J. J.; Crowley, M.; Tsui, V.; Radmer, R. J.; Duan, Y.; Pitera, J.; Massova, I.; Seibel, G. L.; Singh, U. C.; Weiner, P. K.; Kollman, P. A. (1999), AMBER 6, University of California, San Francisco.
- Falgueret, J. P.; Oballa, R. M.; Okamoto, O.; Wesolowski, G.; Aubin, Y.; Rydzewski, R. M.; Prasit, P.; Riendeau, D.; Rodan, S. B.; Percival, M. D. *J. Med. Chem.* **2001**, *44*, 94.
- Ma, D.; Zhang, Y.; Yao, J.; Wu, S.; Tao, F. *J. Am. Chem. Soc.* **1998**, *120*, 12459.
- Saito, K.; Harada, K. *Bull. Chem. Soc. Jpn.* **1989**, *62*, 2562.